Published in final edited form as:
J Immunol. 2010 August 15; 185(4): 2382–2392. doi:10.4049/jimmunol.1000423.

Foxp3+ CD4 Regulatory T Cells Limit Pulmonary Immunopathology by Modulating the CD8 T Cell Response during Respiratory Syncytial Virus Infection

Ross B. Fulton[*], **David K. Meyerholz**[†], and **Steven M. Varga**[*,†]

[*] Department of Microbiology, University of Iowa

[§] Department of Pathology, University of Iowa

[†] Interdisciplinary Graduate Program in Immunology, University of Iowa, Iowa City, IA, 52242

Abstract

Regulatory Foxp3$^+$ CD4 T cells (Tregs) prevent spontaneous inflammation in the lungs, inhibit allergic and asthmatic responses, and contribute to tolerance to inhaled allergens. Additionally, Tregs have previously been shown to suppress the CD8 T cell response during persistent virus infections. However, little is known concerning the role Tregs play in modulating the adaptive immune response during acute respiratory virus infections. We show following acute respiratory syncytial virus (RSV) infection that Foxp3$^+$ CD4 Tregs rapidly accumulate in the lung-draining mediastinal lymph nodes and lungs. BrdU-incorporation studies indicate that Tregs undergo proliferation that contributes to their accumulation in the lymph nodes and lungs. Following an acute RSV infection, pulmonary Tregs modulate CD25 expression and acquire an activated phenotype characterized as CD11a^{hi}, CD44^{hi}, CD43^{glyco+}, ICOS$^+$, and CTLA-4$^+$. Surprisingly, in vivo depletion of Tregs prior to RSV infection results in delayed virus clearance concomitant with an early lag in the recruitment of RSV-specific CD8 T cells into the lungs. Additionally, Treg depletion results in exacerbated disease severity including increased weight loss, morbidity, and enhanced airway restriction. In Treg-depleted mice there is an increase in the frequency of RSV-specific CD8 T cells that co-produce IFN-γ and TNF-α, which may contribute to enhanced disease severity. These results indicate that pulmonary Tregs play a critical role in limiting immunopathology during an acute pulmonary virus infection by influencing the trafficking and effector function of virus-specific CD8 T cells in the lungs and draining lymph nodes. This is an author-produced version of a manuscript accepted for publication in *The Journal of Immunology* (*The JI*). The American Association of Immunologists, Inc. (AAI), publisher of *The JI*, holds the copyright to this manuscript. This version of the manuscript has not yet been copyedited or subjected to editorial proofreading by *The JI*; hence, it may differ from the final version published in *The JI* (online and in print). AAI (*The JI*) is not liable for errors or omissions in this author-produced version of the manuscript or in any version derived from it by the U.S. National Institutes of Health or any other third party. The final, citable version of record can be found at www.jimmunol.org.

[2]Address of correspondence and reprint request to Dr. Steven Varga, Department of Microbiology, 51 Newton Road, 3-532 B.S.B., University of Iowa, Iowa City, IA 52242. address: steven-varga@uiowa.edu.

[1]This work was supported by National Institutes of Health Grant R01 AI063520 to S.M.V. R.B.F. was supported by the Training in Molecular Virology and Viral Pathogenesis Training Grant T32 AI007533 and the Training in Mechanisms of Parasitism Training Grant T32 AI007511.

[3]The online version of this article contains supplemental material.

Keywords

Treg; Lung; Virus; T cells; Rodent

Introduction

The respiratory tract forms a major mucosal interface with the external environment and is constantly exposed to inert foreign antigens and pathogens. Thus, the lungs must discriminate between innocuous and pathogen-derived antigens in order to limit chronic inflammation and maintain proper lung function. To do so, the respiratory system establishes a default anti-inflammatory state that requires a higher activation threshold for pathogen-associated danger signals than non-mucosal surfaces (1). Once the threshold for innate immune activation is exceeded, the immune system must initiate an appropriately balanced immune response that eliminates the pathogen while limiting damage to the lung tissue. Since the lung is not an organized lymphoid tissue, the cellular composition of the lung parenchyma and airways undergoes drastic changes during an immune response (2). Consequently, the lung epithelium is directly exposed to the inflammatory immune response and is therefore susceptible to immune-mediated damage. Thus, failure to tightly regulate the immune response to respiratory pathogens can lead to pulmonary pathology resulting in diminished lung function.

There are multiple regulatory mechanisms in the lungs to control the immune response to respiratory pathogens (1). The initial regulatory barriers in place prior to the induction of an adaptive immune response include active suppression by epithelial cells (3) and alveolar macrophages (4). For instance, exposure of alveolar macrophages to TGF-β that is tethered to airway epithelial cells via the $\alpha_v\beta_6$ integrin serves to maintain macrophages in an anti-inflammatory state and increases the activation threshold of danger signals needed to induce an immune response. Additionally, regulatory CD4 T cells (Tregs) are essential in regulating the adaptive immune response (5,6). Identified by expression of the forkhead transcription factor Foxp3 (7,8), which is required for regulatory function, $Foxp3^+$ Tregs prevent spontaneous inflammation in the lungs (9,10), control atopic and asthmatic responses (11), and have in important role in establishing mucosal tolerance to antigens (5,11). In recent years, it has become appreciated that Tregs also play an important role in regulating immune responses to pathogens (12). The majority of studies examining the role of Tregs during infections have been performed in the context of persistent or chronic infections (13,14). During chronic infections, Tregs have primarily been shown to limit immunopathology mediated by pathogen-specific T cells, and, in some cases, may promote pathogen persistence (15). Importantly, relatively little is known about the role of Tregs during acute virus infections.

To better understand the role of $Foxp3^+$ Tregs during acute respiratory virus infections, we examined the Treg response following acute RSV infection. We show that $Foxp3^+$ Tregs rapidly proliferate and accumulate in the lungs and mediastinal lymph nodes (medLNs) during acute RSV infection. In contrast to Tregs in lymphoid compartments, of which the majority are $CD25^+$, the frequency of $CD25^+$ Tregs in the lungs is modulated following infection. In addition, the majority of pulmonary Tregs upregulate expression of the inhibitory molecule CTLA-4 and acquire an activated phenotype. We demonstrate that Tregs coordinate the early recruitment of virus-specific CD8 T cells into the lung tissue and airways, but also limit the magnitude of the CD8 T cell response and their ability to produce TNF-α, which likely reduces disease severity. Our data indicate that Tregs play an important role in the regulation of the adaptive CD8 T cell response that is the primary cause of RSV-induced lung immunopathology.

Materials and Methods

Viruses and infection of mice

The A2 strain of RSV was a gift from B. S. Graham (National Institutes of Health; NIH, Bethesda, MD) and was propagated on HEp-2 cells (American Type Culture Collections; ATCC, Manassas, VA). BALB/cAnNCr mice between the ages of 6-8 weeks were purchased from the National Cancer Institute (Bethesda, MD). Mice were anesthetized with isofluorane and infected with 2-3 × 10^6 PFU of the A2 strain of RSV intranasally (i.n.). All experimental procedures were approved by the University of Iowa's Animal Care and Use Committee.

Tissue isolation and preparation

The bronchoalveolar lavage (BAL) fluid and lung tissue were harvested from mice as previously described (16). After perfusing the lungs with 5 ml of PBS via the right ventricle of the heart, lungs were cut into small pieces and digested in 4 ml of HBSS with $CaCl_2$ and $MgCL_2$ (Gibco, Grand Island, NY) supplemented with 125 U/ml collagenase (Invitrogen, Carlsbad, CA) and 60 U/ml DNase I (Sigma, St. Louis, MO) for 30 min at 37°C. Lymph nodes were similarly digested in 1 ml of HBSS containing collagenase and DNase I as described above. Lungs were then pressed through a wire mesh screen (Cellector; Bellco Glass, Inc., Vineland, NJ) and spleens and lymph nodes were pressed between the frosted ends of glass slides (Surgipath, Richmond, IL) to prepare single-cell suspensions.

Cell Surface Staining

Single-cell suspensions (1 × 10^6 to 2 × 10^6 cells) were plated in 96-well round-bottom plates (Corning Inc., Corning, NY) and blocked with anti-FcγRII/III monoclonal antibody (mAb) (clone 93) and simultaneously stained with optimal concentrations of mAbs specific for CD4 (clone RM4.5), CD8 (clone 53-6.7), Thy1.2 (clone 53-2.1), CD25 (clone PC61.5), CD45RB (clone C363.16A), CD11a (clone M17/4), CD44 (clone IM7), CD43 (glycosylated; clone 1B11), CD69 (clone H1.2F3), glucocorticoid-induced TNFR-related protein (GITR; clone DTA-1), OX40 (clone OX-86), ICOS (clone 7E.17G9), CD62L (clone MEL-14), CD103 (clone M290), β7 (clone M293), and CD49d (clone R1-2). All mAbs were obtained from eBioscience (San Diego, CA) except for CD43, CD103, and β7, which were obtained from BD Biosciences (San Jose, CA). Cells were stained for 30 min at 4°C, washed twice with cold staining buffer (PBS, 2% FCS, and 0.02% sodium azide), and subsequently fixed with FACS lysing solution (BD Biosciences). Samples were run on a Becton Dickinson FACSCanto flow cytometer and data were analyzed using FlowJo software (Tree Star Inc., Ashland, OR).

Tetramer staining

Cells were plated in 96-well round-bottom plates (Corning Inc., Corning, NY), washed with staining buffer, and stained with optimal concentrations of RSV $M2_{82-90}$-specific allophycocyanin-conjugated tetramers (obtained from the NIH Tetramer Core Facility, Atlanta, GA) and simultaneously blocked with anti-FcγRII/III mAb for 30 min at 4°C. Cells were washed once with cold staining buffer, stained for cell surface CD8 and Thy1.2, and subsequently washed and fixed with FACS lysing solution prior to analysis by flow cytometry.

Intracellular staining and BrdU

Cells were stained for Foxp3 using the mouse regulatory T cell staining buffer kit (eBioscience) according to the manufacturer's instructions. Briefly, following cell surface staining and fixation, cells were stained with optimal concentrations of mAb specific to

Foxp3 (clone FJK-16s; eBioscience), CTLA-4 (clone UC10-4B9; eBioscience), and Ki-67 (clone 35; BD Biosciences). Cells were subsequently washed twice with 1X permeabilization buffer and resuspended in staining buffer. For BrdU studies, mice were administered 2 mg BrdU (Sigma) intraperitoneally (i.p.) and 0.8 mg i.n. in pharmaceutical grade PBS (Gibco) 24 hrs prior to analysis. To detect BrdU incorporation, cells were first stained for Foxp3 followed by intracellular BrdU staining with mAb specific to BrdU (clone PRB-1; eBioscience) using the BrdU Flow kit (BD Biosciences) according to the manufacturer's instructions. DNase I for BrdU staining was obtained from Sigma. Samples were analyzed using flow cytometry.

In vivo depletion of Tregs

Hybridoma cells producing anti-CD25 mAb (clone PC61) were a gift from Thomas Waldschmidt (University of Iowa). Anti-CD25 mAb was produced in CELLine CL 1000 chambers (Integra, Hudson, NH) using HyClone SFM4MAb w/L-Glutamine media (Thermo Fisher Scientific, Waltham, MA) according to the manufacturer's instructions. Anti-CD25 mAb was purified using a 50% ammonium sulfate precipitation and dialyzed with pharmaceutical-grade PBS. To deplete $CD25^+$ CD4 T cells, naïve BALB/c mice were administered 1 mg anti-CD25 mAb (PC61) i.p. 3 days prior to infection. Mice were subsequently infected with RSV i.n. and administered 500 μg anti-CD25 mAb i.p. 2 days later. Control mice were administered the same amount of rat IgG (Sigma) in parallel with anti-CD25 mAb treatments. To confirm depletion of $CD25^+$ CD4 T cells, cells were stained for cell surface CD4, Thy1.2, CD25 (clone 7D4; eBioscience), and intracellular Foxp3. The 7D4 clone does not recognize the same epitope on CD25 as the PC61 mAb used for depletion (17).

Peptide stimulation

Single-cell suspensions derived from the spleen, medLNs, lung, and BAL fluid were plated in 96-well round-bottom plates (Corning Inc.) for 5 hr at 37°C with or without 1 μM of $M2_{82\text{-}90}$ peptide in the presence of 10 μg/ml brefeldin A (Sigma) as previously described (16). Cells were subsequently stained for cell surface CD8 and Thy1.2. After fixation with FACS lysing solution, cells were incubated in permeabilization buffer (staining buffer containing 0.5% saponin; Sigma) for 10 min and stained with optimal concentrations of anti-IFN-γ clone XMG1.2; eBioscience) and anti-TNF-α (clone MP6-XT22; eBioscience). Cells were washed once with permeabilization buffer and again with staining buffer prior to analysis by flow cytometry.

Measurement of morbidity and airway resistance

Enhanced pause (Penh) was measured using a whole body plethysmograph (Buxco Electronics, Sharon, CT). Penh values were recorded daily prior to and following infection with RSV. Breathing patterns were recorded for 5 minutes per mouse to obtain an average Penh value. Mice were weighed daily and clinical scores were assigned based on the following scale: 0, no apparent illness; 1, slightly ruffled fur; 2, ruffled fur; 3, ruffled fur and inactive; 4, ruffled fur, inactive, hunched posture; and 5, moribund or dead.

Plaque assays

Lungs were harvested from RSV-infected mice on days 4, 6, and 7 postinfection (p.i.) and processed for plaque assays on Vero cells as previously described (18).

Histology

Whole lungs with the heart attached were removed from control or Treg-depleted mice 7 days p.i. Lungs were placed in 10% formalin (Thermo Fisher Scientific) in a vacuum to

remove air from the lungs. Fixed lungs were embedded in paraffin, sectioned at 4 μm thickness, and either H&E or periodic acid-Schiff (PAS) stained by the University of Iowa Comparative Pathology Laboratory. Slides were blinded and scored by a board-certified veterinary pathologist (D. Meyerholz, University of Iowa, Iowa City, IA). Stained sections were scored for perivascular aggregates of leukocytes (PVA) from 1 to 4 on a graded scale in which 1 represents normal parameters and 4 represents moderate to high cellularity. Interstitial disease was scored on the following scale: 1, within normal parameters; 2, mild, detectable focal to multifocal congestion, uncommon to small numbers of leukocytes and some atelectasis; 3, moderate, multifocal to coalescing congestion, leukocyte cellularity, and atelectasis with rare luminal leakage of cellular and fluid debris; 4, Severe, coalescing interstitial congestion, leukocytes, and atelectasis with admixed extensive of loss of airspace and luminal accumulation of cellular and fluid debris. Edema was scored from 1 to 4 on a graded scale in which 1 represents no edema and 4 represents multiple fields having coalescing alveoli filled by pools of fluid. Mucus airway obstruction was scored on the following scale: 1, normal epithelium and no luminal accumulation; 2, epithelial mucinous hyperplasia with thin strands of mucus lining the airways; 3, epithelial mucinous hyperplasia with luminal mucus accumulation partially filling the airways; 4, epithelial mucinous hyperplasia with luminal mucus filling and obstructing the airways.

Data analysis

Graphical analysis was performed using Prism software (Graphpad Software Inc., San Diego, CA). Statistical analyses were performed using InStat software (Graphpad Software, Inc.). Comparisons between two groups with normal Gaussian distributions were analyzed using paired or unpaired *t* tests (two-tailed), a Welch corrected unpaired *t* test for data with significant differences in SD between groups, or a Mann-Whitney *U* test for data without Gaussian distributions. Within group comparisons to baseline were analyzed using a one-way ANOVA with a Dunnett post-test to control for multiple comparisons. Overall trends in longitudinal data between groups were analyzed using two-way repeated-measures ANOVA. *P* values were considered significant when $p<0.05$.

Results

Foxp3$^+$ Tregs rapidly accumulate in the lungs and medLNs during RSV infection

Treg responses to pathogens have been extensively studied in the context of persistent or chronic infections (13–15,19,20). In contrast, much less is known concerning the role of Tregs during acute infections (21). Following acute infection of BALB/c mice with RSV, the frequency of CD4 T cells that were Foxp3$^+$ increased in the lung airways (BAL), lung parenchyma, and lung-draining medLNs (Fig. 1A-C). By day 4 p.i., 25% of CD4 T cells in the BAL were Foxp3$^+$, representing a ~50-fold increase in absolute numbers over naïve levels (Fig. 1A). By day 8 p.i., the total number of Tregs in the BAL had increased 86-fold over naïve levels. The lung parenchyma also exhibited an increase in the frequency and total number of Tregs (Fig. 1B). By day 6 p.i. the frequency of CD4 T cells that were Foxp3$^+$ more than doubled compared to naïve levels (17% compared to 7%) which represented a ~3-fold increase in total numbers of Tregs over naïve levels. Thus, following infection with RSV there was an early enrichment of Tregs in the BAL and lung parenchyma. In contrast, the frequency of Foxp3$^+$ CD4 T cells in the medLNs remained relatively constant except for an early increase on day 2 p.i. (Fig. 1C). However, the absolute number of Tregs rapidly increased during the first several days p.i., indicating that the accumulation of Tregs paralleled that of Foxp3$^-$ CD4 T cells (data not shown). In contrast to the lungs and medLNs, we did not observe large fluctuations in the frequency or total number of Foxp3$^+$ CD4 T cells in the spleen or PBL (Figs. 1D and E).

Concomitant with clearance of RSV from the lungs by day 7 p.i. (22), the number of Tregs decreased in the BAL, lung parenchyma, medLNs, and spleen (Figs 1A-D). By day 15 p.i., absolute number of Tregs in the lung parenchyma and spleen had nearly returned to baseline levels. The decline in Treg numbers was more prolonged in the BAL and medLNs, but total numbers were similar to baseline levels at day 220 p.i. We observed an increase in the frequency of $Foxp3^+$ CD4 T cells in the medLNs and spleen by day 220 p.i. along with increased Treg numbers in the spleen (Figs. 1C and D), which is consistent with studies showing an increase in $Foxp3^+$ Tregs in mice as they age (15,23). The kinetics of the Treg response to RSV infection was not unique to BALB/c mice; we observed similar kinetics in the BAL, lung parenchyma, medLNs, spleen, and PBL following acute RSV infection of C57BL/6 $Foxp3^{gfp}$ mice (data not shown).

Proliferation of $Foxp3^+$ Tregs during RSV infection

The accumulation of $Foxp3^+$ Tregs in the medLNs and lungs during RSV infection could be explained by the recruitment and/or proliferation of Tregs. To determine if Tregs proliferate in response to RSV infection, we examined BrdU incorporation in parallel with the proliferation marker Ki-67. Twenty-four hrs prior to analysis, naïve or RSV-infected BALB/c mice were administered BrdU both i.p. and i.n. to ensure efficient incorporation of BrdU by proliferating cells in the lung parenchyma and BAL (24). Consistent with previous reports (11,25,26), prior to infection the percentage of Tregs that were $Ki\text{-}67^+$ or $BrdU^+$ was significantly higher than conventional $Foxp3^-$ CD4 T cells ($p<0.01$ for all except Ki-67 frequencies in the BAL) (Fig. 2). Following RSV infection, there was an increase in the frequency of proliferating Tregs in the BAL, lung parenchyma, medLNs, and spleen compared to naïve controls. By day 6 p.i., 78% and 69% of Tregs in the BAL and lung parenchyma, respectively, were $Ki\text{-}67^+$. In the spleen there was a much smaller increase over naïve levels relative to the lungs and medLNs (Fig. 2D). By day 15 p.i. the frequency of proliferating Tregs in the lungs, medLNs, and spleen had decreased to levels comparable to naïve mice. Due to the relatively short 24 hr BrdU pulse, we consistently observed higher frequencies of $Ki67^+$ compared to $BrdU^+$ CD4 T cells. Interestingly, we observed a higher percentage of $Foxp3^+$ Tregs undergoing proliferation as compared to $Foxp3^-$ CD4 T cells at all times examined. These results demonstrate that RSV infection induces local proliferation of Tregs that contributes to the accumulation of $Foxp3^+$ Tregs in the BAL, lung parenchyma, and medLNs.

CD25 expression by $Foxp3^+$ Tregs during RSV infection

Since Tregs were proliferating and presumably becoming activated in response to RSV infection, we next wanted to examine the phenotype of pulmonary Tregs following infection. Although IL-2 is essential for the peripheral maintenance of Tregs (27,28), it has previously been shown that while the majority of $Foxp3^+$ CD4 T cells are $CD25^+$ in secondary lymphoid tissues, this frequency is decreased in the lungs (29). To determine if CD25 was modulated during the course of infection, we tracked CD25 expression by $Foxp3^+$ Tregs (Fig. 3). The frequencies of $CD25^+$ $Foxp3^+$ Tregs in the medLNs and spleen remained relatively stable at ~80% throughout the course of infection (Fig. 3). As expected, in naïve mice 59% of Tregs in the lung parenchyma were $CD25^+$. In contrast, 74% of Tregs in the BAL of naïve mice were $CD25^+$, suggesting that Tregs in the lung airways may up-regulate CD25 expression or that $CD25^+$ Tregs are preferentially recruited to or retained in the airways. Following infection, the percentage of $CD25^+$ Tregs in the lung parenchyma dipped to 50% and remained relatively stable afterwards. In contrast to the lung parenchyma, ~70–75% of Tregs in the BAL remained $CD25^+$ during the first 8 days of infection. The frequency then decreased to 54% by day 15 p.i. before eventually returning to baseline levels by day 220.

Pulmonary Tregs acquire an activated phenotype during RSV infection

To further assess the activation phenotype of Tregs, we compared pulmonary Tregs from naïve or RSV-infected mice for markers commonly associated with T cell activation. Consistent with previous reports that Tregs from naïve mice display an effector cell phenotype (17,30), >90% of pulmonary Tregs were CD45RB^{low} and ~40% were high for the memory markers CD11a and CD44 (Fig. 4). Approximately 40% of Tregs expressed the activation-associated glycoform of CD43 (CD43^{glyco}) and the costimulatory receptor ICOS, suggesting that some Tregs may have been recently activated. A low frequency (<4%) of Tregs expressed CD69 and OX40 and >90% were GITR^{hi} and FR4^{hi} (Supplemental Fig. 1). CTLA-4 is an inhibitory homolog of CD28 that is constitutively expressed by a portion of Tregs and has been implicated as a regulatory mechanism used by Tregs (9,31–33). In the lung parenchyma, 37% of Tregs were CTLA-4^{+}. Few Tregs expressed the inhibitory molecules LAG-3, programmed death 1 (PD-1), or programmed death ligand (PDL)-2 (data not shown). However, 15% of Foxp3^{+} Tregs expressed PDL-1 (Supplemental Fig. 1).

By day 6 p.i., pulmonary Tregs further down-regulated CD45RB expression, 70–80% became CD11a^{hi} and CD44^{hi}, and there was a ~2.5-fold increase in the geometric mean fluorescence intensity (MFI) of GITR compared to Tregs from the lung parenchyma of naïve mice (Fig. 4 and data not shown). We also observed a significant (p<0.01) increase in the frequency of Tregs expressing CD43^{glyco} (70%), ICOS (81%), CTLA-4 (78%), CD69 (34%), OX40 (21%), and PDL-1 (62%) compared to Tregs from the lungs of naïve mice (Fig. 4 and Supplemental Fig. 1). There were minimal changes in LAG3, PD-1, and PDL-2 expression (data not shown). These data further demonstrate that pulmonary Tregs are highly activated during acute RSV infection.

Pulmonary Tregs modulate trafficking molecules during infection

We also examined the modulation of trafficking molecules on pulmonary Tregs. In naïve mice, 23% of pulmonary Tregs had low expression of CD62L (Fig. 5). By day 6 p.i., 54% of Tregs in the lung parenchyma had low CD62L expression. The $\alpha_E\beta_7$ integrin has been shown to be important for Treg trafficking to sites of inflammation such as the skin and lungs (30,34). The frequency of α_E- and β_7-expressing Tregs in the lung parenchyma increased from 30% and45%, respectively, in naïve mice to 40% and 67%, respectively, by day 6 p.i. (Fig. 5). Compared to Foxp3^{-} CD4 T cells, expression of the α_E and β_7 integrin chains were primary restricted to Foxp3^{+} CD4 T cells, suggesting that $\alpha_E\beta_7$ may be important for Treg trafficking into the lungs during RSV infection. Additionally, the $\alpha_4\beta_1$ integrin (VLA-4) has been demonstrated to be important for trafficking of lymphocytes into bronchus-associated lymphoid tissue via VCAM-1 expressed on high endothelial venules (35). We observed an increase in the frequency of both Foxp3^{+} Tregs and Foxp3^{-} CD4 T cells expressing high levels of the α_4 integrin chain. Thus, the α_4 integrin chain may also be important in trafficking of both Treg and effector CD4 T cells into the lungs.

Depletion of Tregs delays virus clearance

Depletion of Tregs has been shown in most infection models to accelerate pathogen clearance due to enhanced T cell responses (13–15,36). Therefore, we next determined if depletion of Tregs altered the rate of virus clearance in the lungs. Naïve mice were treated with anti-CD25 mAb 3 days prior to RSV infection and a second time 2 days p.i. to ensure sustained depletion of CD25^{+} Tregs. At the time of infection, in the lung parenchyma there was an ~86% reduction in the percentage of Foxp3^{+} Tregs that were CD25^{+} as detected by the anti-CD25 mAb clone 7D4 (Supplemental Fig. 2A). This decrease corresponded with a ~60% reduction in the frequency of Foxp3^{+} CD4 T cells, consistent with the depletion of this population (Supplemental Fig. 2B). The residual frequency of Foxp3^{+} Tregs was expected based on our previous observation that only 59% of Tregs in the lung express

CD25 (Fig. 3). There were similar virus titers on days 4 and 6 p.i. in the lungs of control and Treg-depleted mice (Fig. 6). However, despite only being able to eliminate 60% of the Tregs in the lung via anti-CD25-mediated depletion, we observed a significant ($p<0.01$) delay in virus clearance (Fig. 6). These data suggest that the virus-specific CD8 T cell response, which is necessary to mediate clearance of RSV (37,38), might be negatively impacted when Treg numbers are reduced during infection.

Depletion of CD25$^+$ Tregs delays the recruitment of RSV-specific CD8 T cells into the lung

Multiple studies have shown that Tregs limit the magnitude of pathogen-specific CD8 T cell responses (13,21,39,40), which would appear to be at odds with our data demonstrating that virus-clearance is delayed in Treg-depleted mice. Therefore, we next sought to examine the impact of Treg depletion on the magnitude and kinetics of the RSV-specific CD8 T cell response. Consistent with the role of Tregs in limiting overall inflammation, there were significantly ($p<0.01$) more total cells in the lung parenchyma of Treg-depleted mice at both days 6 and 8 p.i. (Fig. 7A). Total cell numbers in the BAL and medLNs were similar between groups on both days examined. On days 6 and 8 p.i. there were increased numbers of CD4 T cells in the lung parenchyma and on day 8 p.i. there were more CD8 T cells in the lung parenchyma and medLNs (Figs. 7B and C). There were also substantially more NK cells ($CD3^-DX5^+$) 6 days p.i. and more B cells ($CD19^+B220^+$) and neutrophils ($Ly6C^+Ly6G^+CD11b^+$) 8 days p.i. in the lung parenchyma of Treg-depleted mice (Fig. 7D).

To determine the effect of Treg depletion on the RSV-specific CD8 T cell response, we enumerated antigen-experienced $CD11a^{hi}CD44^{hi}$ CD8 T cells in the medLNs, lung parenchyma, and BAL (Fig. 8A) (41). In Treg-depleted mice there were significantly ($p<0.01$) more $CD11a^{hi}CD44^{hi}$ CD8 T cells in the medLNs on days 6 and 8 p.i. In contrast, there were significantly ($p<0.05$) fewer $CD11a^{hi}CD44^{hi}$ CD8 T cells in the lung parenchyma on day 6 p.i. However, by day 8 there was a ~1.6-fold increase in the number of antigen-experienced CD8 T cells compared to control mice. This increase was reflective of the ~1.6-fold increase in total CD8 T cells (Fig. 7C). There was no statistical difference observed in the BAL between control and Treg-depleted mice.

We next examined the immunodominant $M2_{82\text{-}90}$ CD8 T cell response. On day 6 p.i. there were similar frequencies and numbers of $M2_{82\text{-}90}$ tetramer-specific CD8 T cells in the medLNs of Treg-depleted mice compared to controls (Fig. 8B). However, following *ex vivo* $M2_{82\text{-}90}$ peptide stimulation, we observed a higher percentage of IFN-γ^+ CD8 T cells in the medLNs of Treg-depleted mice (4.4±0.3% in IgG-treated compared to 6.6±0.6% in PC61-treated mice; $p<0.01$) at day 6 p.i. The discrepancy in frequencies of $M2_{82\text{-}90}$-specific CD8 T cells in the medLNs at day 6 p.i. as measured by tetramer or IFN-γ is likely a result of decreased tetramer binding to newly activated T cells due to rearrangement of surface T cell receptors (42). As indicated by the decrease in $CD11a^{hi}CD44^{hi}$ CD8 T cells, there was a significant ($p<0.01$) decrease in both the frequency and total number of $M2_{82\text{-}90}$ tetramer-specific CD8 T cells in the lung parenchyma of Treg-depleted mice at day 6 p.i. (Fig. 8B). We observed similar differences in the lung parenchyma and BAL in the percentage of IFN-γ^+ CD8 T cells following *ex vivo* peptide stimulation (data not shown). These data suggest that there is impaired egress of $M2_{82\text{-}90}$ -specific CD8 T cells from the lung-draining LNs into the lungs. Importantly, these data argue against the possibility of non-specific depletion of activated CD8 T cells that have upregulated CD25 expression as the cause of the decrease in the $M2_{82\text{-}90}$-specific CD8 T cell response in the lungs. Furthermore, we observed similar frequencies and total numbers of $M2_{82\text{-}90}$-specific IFN-γ^+ CD8 T cells in the spleen at day 6 p.i. (Fig. 8C and data not shown). By day 8 p.i. in Treg-depleted mice, total numbers of $M2_{82\text{-}90}$ tetramer-specific CD8 T cells were similar to (BAL) or exceeding (lung parenchyma and medLNs) those of control mice, which is in agreement with evidence that Tregs limit the magnitude of the CD8 T cell response (21,39,40). These data suggest that

Tregs are important in coordinating early trafficking of virus-specific CD8 T cells into the lung parenchyma and airways.

Tregs limit disease severity during RSV infection

Given the altered kinetics of CD8 T cell accumulation in the lung, we next assessed morbidity in Treg-depleted mice. Compared to control mice, Treg-depleted mice exhibited increased clinical illness on days 7 and 8 p.i. (Fig. 9A) accompanied with increased weight loss (Fig. 9B). We used whole body plethysmography to determine if depletion of Tregs resulted in increased enhanced pause (Penh) during RSV infection (Fig. 9C). Mice depleted of Tregs exhibited a delayed rise in Penh compared to control mice. Increased Penh values were sustained in Treg-depleted mice that could not be simply accounted for by a single day delay (day 8 Treg-depleted vs. day 7 control, p=0.002; day 9 Treg-depleted vs. day 8 control, p=0.02). These data indicated that depletion of Tregs results in increased airway resistance during infection. Lungs from Treg-depleted mice had increased severity of perivascular aggregates of leukocytes that primarily consisted of lymphocytes (Fig. 10). Compared to control mice, the lung airways of Treg-depleted mice also had more severe epithelial mucinous hyperplasia with luminal mucus filling and obstructing the airways. Thus, Treg depletion results in increased disease during the late immune phase that coincides with the adaptive immune response.

Depletion of Tregs enhances TNF-α production by CD8 T cells

The exacerbated disease severity observed in Treg-depleted mice during RSV infection could be explained by delayed virus clearance and/or enhanced T cell-mediated immunopathology. In Treg-depleted mice, CD8 T cells could contribute to enhanced disease by producing increased amounts of the pro-inflammatory cytokine TNF-α. TNF-α has been shown to be a major cause of illness during acute RSV infection (43). Following *ex vivo* peptide stimulation, higher frequencies of $M2_{82\text{-}90}$-specific CD8 T cells from Treg-depleted mice were capable of co-producing IFN-γ and TNF-α relative to control mice (Figs. 11A and B). Compared to control mice, a higher frequency of CD8 T cells isolated from the lung parenchyma and BAL of Treg-depleted mice co-produced IFN-γ and TNF-α on day 6 p.i. and from the medLNs on both 6 and 8 days p.i. The MFI of TNF-α in Treg-depleted mice was substantially higher than in control mice; there was a ~1.5-fold and ~1.9-fold increase in the TNF-α MFI in the lung parenchyma and BAL, respectively, on day 6 p.i. (Figs. 11A and C). In the medLNs there was a ~1.7-fold increase in TNF-α MFI on both 6 and 8 days p.i. Consequently, increased *in vivo* production of TNF-α in Treg-depleted mice would likely contribute to enhanced disease.

Discussion

The majority of studies examining $Foxp3^+$ Tregs during immune responses to pathogens have focused on pathogens that establish chronic infections (13,14). Since depletion of Tregs prior to acute infection with lymphocytic choriomeningitis virus, the most widely studied virus in viral immunology, did not appear to affect the CD8 T cell response (13), much of the focus has remained on chronic infection models. Regardless of the reasons, much less is known about the Treg response to pathogens during acute infections.

In order to characterize the activation state of Tregs during acute RSV infection, we examined a broad panel of T cell activation markers. Given that IL-2 is crucial for the maintenance of Tregs in the periphery (27), it is curious that roughly half of $Foxp3^+$ Tregs in the lungs do not express CD25. The high-affinity IL-2R is comprised of CD25 (IL-2Rα), CD122 (IL-2Rβ), and CD132 (common γ– chain). While IL-2 can still signal through the low-affinity IL-2 receptor comprised of the IL-2Rβ and γc chains, the low-affinity IL-2R is

not sufficient for peripheral Treg maintenance as IL-2 or CD25 deficient mice have a drastic reduction in the frequency of peripheral Tregs and suffer from severe autoimmunity (27,28). After IL-2 binds the IL-2R, the complex is internalized and CD25 is recycled back to the cell surface. Since ~20% of Foxp3$^+$ Tregs do not express CD25 at any given time, this may reflect a population of Tregs that recently bound IL-2. Thus, the high frequency of Tregs in the lung that do not express CD25 may reflect cells that recently received IL-2 signals.

Additional analysis of activation-associated molecules on Tregs during infection revealed that the vast majority of Tregs in the lungs exhibited an activated phenotype (CD11a^{hi}, CD44^{hi}, CD43^{glyco+}, ICOS$^+$, CTLA-4$^+$) and had upregulated expression of the α_4 and β_7 integrin chains. Relative to the Foxp3$^+$ Treg population, the frequency of Foxp3$^-$ CD4 T cells expressing these molecules was notably reduced. This is perhaps not unexpected since the conventional CD4 T cell response is likely made up of a diverse array of differentiated subsets and memory CD4 T cells non-specifically recruited into the lung. However, it has been suggested that some of the markers expressed by Tregs identify distinct populations with different inhibitory mechanisms or trafficking profiles. For instance, it has been suggested that expression of the α_E integrin chain or the costimulatory receptor ICOS may identify two functionally distinct subsets of Foxp3$^+$ Tregs (30,34,44–46). Following RSV infection, the majority of Tregs in the lung parenchyma and BAL (data not shown) upregulated CTLA-4. Recent studies have shown that CTLA-4 expressed by Foxp3$^+$ Tregs is required to maintain systemic tolerance (9,31). However, in the context of an infection, it is unknown if Treg-specific expression of CTLA-4 is required to regulate T cell activation or if CTLA-4 expressed by non-regulatory T cells is sufficient. Since effector T cells also express CTLA-4 during infection, it is less clear to what extent CTLA-4 expressed by Tregs regulates T cell activation and proliferation. Further studies using CTLA-4 conditional knockout mice lacking CTLA-4 in Foxp3$^+$ Tregs would help elucidate the role of Treg-associated CTLA-4 during RSV infection.

While our data revealed that Tregs are activated during RSV infection, it is not clear what signals induce the activation of Tregs. This is especially unclear for natural Tregs (nTregs), which are believed to recognize self-antigens (14,47). If one assumes that the majority of the Foxp3$^+$ Tregs responding to RSV infection are nTregs, there are several possible ways to explain their activation (13). One possibility is that nTregs recognize tissue-specific antigens in the context of non-tolerogenic inflammation caused by the infection. Another possibility is that nTregs recognize pathogen-derived antigens. However, there is little evidence that there is broad cross-reactivity between pathogen- and self-derived antigens. Furthermore, since Tregs have been shown to respond to a wide variety of pathogens, the majority of which establish chronic infections, cross-reactivity would have to be the rule rather than the exception. In a third scenario, nTregs maybe non-specifically activated through recognition receptors such as Toll-like receptors (TLRs) or cytokines such as type I interferons. Tregs express multiple toll-like receptors (TLRs) including TLR4, 5, 7, and 8 (48). This may be an intriguing possibility in the case of RSV infection since the RSV F protein has been shown to induce TLR4 signaling (49).

During certain conditions, antigen-specific adaptive Foxp3$^+$ CD4 Tregs (aTregs) can be generated the periphery (5). Evidence for the development of aTregs is strongest at mucosal sites such as the intestinal tract and the lungs (5,11,50). For instance, intranasal delivery of antigen results in the conversion of conventional Foxp3$^-$ CD4 T cells into adaptive Foxp3$^+$ Tregs that can prevent allergic inflammation (11,51). In response to pathogens, the generation of aTregs has been shown during persistent infections where antigen may be present in subimmunogenic conditions with low levels of inflammatory cytokines or low expression of costimulatory molecules (5). In contrast, acute infections may not provide the right type of environment that would require the additional regulation provided by aTregs

(12). One major confounding issue in studying aTregs and nTregs is the lack of phenotypic markers to distinguish between the two populations. Consequently, in our studies we were unable to determine if adaptive Foxp3$^+$ Tregs were contributing to the overall Treg response during acute RSV infection. There is evidence that a small frequency of Foxp3$^+$ Tregs in the lungs is RSV-specific as determined by tetramers (52). However, since the frequency of RSV-specific tetramer$^+$ CD4 T cells identified in this study was small (<1% of the total CD4 T cells in the lung), it is difficult to extrapolate what fraction of Foxp3$^+$ Tregs are RSV-specific. Unfortunately, without the ability to identify a larger proportion of RSV-specific CD4 T cells by tetramer and the lack of RSV-specific TCR transgenic mice, it is currently difficult to directly assess the generation of adaptive Foxp3$^+$ Tregs following acute RSV infection.

Foxp3$^+$ Tregs are commonly implicated in the suppression of the adaptive immune response to pathogens as a way to limit immunopathology. However, there is evidence that Tregs coordinate innate and adaptive immune responses to pathogens. Tregs have been reported to promote the trafficking of effector immune cells to the primary site of infection during genital HSV-2 infection (53) and in CB6F1 hybrid mice during RSV infection (21). Conversely, Tregs may also be able to block trafficking by inhibiting expression of chemokine receptors (54). During RSV infection in Treg-depleted CB6F1 mice, there was a significant lag in the $D^bM_{187\text{-}195}$-specific CD8 T cell responses in the lungs compared to control mice. This lag in the virus-specific T cell response corresponded with decreased virus clearance in the lungs on days 6 and 7 p.i. Our study substantiates this role of the Treg response in the BALB/c model. Importantly, our data offers the novel observation that there is an early accumulation of RSV-specific CD8 T cells in the lung-draining medLNs of Treg-depleted mice, suggesting that there is delayed egress out of the medLNs into the lungs. These findings suggest that Tregs help coordinate the early trafficking of activated CD8 T cells from the draining LNs into the lungs. Tregs may influence expression of chemokines in the lungs or chemokine receptors on virus-specific CD8 T cells. During RSV infection, CXCL10 has been shown to be important for the recruitment of virus-specific CD8 T cells into the lungs (55). Initial experiments did not reveal obvious differences in the chemokines CXCL9, CXCL10, CXCL11, CCL3, and CCL5 in the lung parenchyma and BAL as a whole (data not shown), but there may be more subtle differences in chemokines produced by specific immune cell populations. Alternatively, Tregs could influence expression levels of sphingosine 1-phosphate receptor-1 on CD8 T cells in the draining LNs, delaying their egress from the draining LNs into the lung. Our laboratory is currently examining these possibilities.

Much of what is known about RSV-induced pathogenesis comes from studies in the BALB/c mouse model (37,56). In this study we demonstrated that depletion of CD25$^+$ Tregs prior to infection exacerbated disease severity. Given that we were only able to deplete ~60% of Foxp3$^+$ Tregs, we believe that our results represent an underestimate of the overall effect that Tregs have in limiting pulmonary immunopathology. This study uniquely demonstrates that increased *in vivo* production of TNF-α by RSV-specific CD8 T cells could contribute to increased morbidity in Treg-depleted mice. While there was no major increase in TNF-α production by CD8 T cells reported in Treg-depleted CB6F1 mice during RSV infection (21), we observed notable increases in *ex vivo* production of TNF-α by CD8 T cells in the lungs and medLNs of Treg-depleted mice. While there were lower total numbers of $M2_{82\text{-}90}$-specific CD8 T cells in the lungs day 6 p.i., this increase translated into significantly ($p<0.001$) more total numbers of $M2_{82\text{-}90}$-specific CD8 T cells capable of co-producing IFN-γ and TNF-α in the medLNs, a trend toward increased total numbers in the spleen ($p=0.06$), and similar numbers in the lung (data not shown). Additionally, increased per cell production of TNF-α in Treg-depleted mice as indicated by MFI could further account for CD8 T cell-mediated disease.

RSV is the leading cause of severe lower respiratory virus infections in infants and is the second leading cause of virus-induced respiratory disease in the elderly and adults with chronic cardiopulmonary disorders or who are immunocompromised (57,58). While CD8 T cells are important in RSV clearance from the lungs, they may also contribute to disease pathology (59), although to what extent remains controversial (58). In addition to inhibiting autoimmunity to self-antigens, it is increasingly evident that $Foxp3^+$ Tregs have an important role in regulating the adaptive immune response to pathogens (12). By better understanding the function of Tregs during acute respiratory virus infections, we will gain further insight of the mechanisms in place to regulate virus-specific T cell responses. This may lead to the ability of the T cell response to be manipulated to optimize virus clearance while minimizing immunopathology. It will be important to further expand these studies to other respiratory pathogens to better understand host-pathogen interactions and how Tregs regulate the immune response.

Supplementary Material

Refer to Web version on PubMed Central for supplementary material.

Acknowledgments

The authors would like to thank Kevin Legge for critical review of the manuscript and Elizabeth Dastrup and Kathryn Chaloner for assistance with the statistical analyses. We also thank Stacey Hartwig for her excellent technical assistance.

Abbreviations used in this paper

aTreg	adaptive regulatory T cell
BAL	bronchoalveolar lavage
GITR	glucocorticoid-induced TNF-related protein
glyco	glycofform
ID	interstitial disease
i.n	intranasal(ly)
medLN	mediastinal lymph node
MFI	mean fluorescence intensity
nTreg	natural regulatory T cell
PAS	periodic acid Schiff
PD-1	programmed death 1
Penh	enhanced pause
p.i	postinfection
PVA	perivascular aggregates of leukocytes
RSV	respiratory syncytial virus
Treg	regulatory T cell

References

1. Holt PG, Strickland DH, Wikstrom ME, Jahnsen FL. Regulation of immunological homeostasis in the respiratory tract. Nat Rev Immunol. 2008; 8:142–152. [PubMed: 18204469]

2. Wissinger EL, Saldana J, Didierlaurent A, Hussell T. Manipulation of acute inflammatory lung disease. Mucosal Immunol. 2008; 1:265–278. [PubMed: 19079188]
3. Raz E. Organ-specific regulation of innate immunity. Nat Immunol. 2007; 8:3–4. [PubMed: 17179960]
4. Lambrecht BN. Alveolar macrophage in the driver's seat. Immunity. 2006; 24:366–368. [PubMed: 16618595]
5. Curotto de Lafaille MA, Lafaille JJ. Natural and adaptive foxp3$^+$ regulatory T cells: more of the same or a division of labor? Immunity. 2009; 30:626–635. [PubMed: 19464985]
6. Kim JM, Rasmussen JP, Rudensky AY. Regulatory T cells prevent catastrophic autoimmunity throughout the lifespan of mice. Nat Immunol. 2007; 8:191–197. [PubMed: 17136045]
7. Hori S, Nomura T, Sakaguchi S. Control of regulatory T cell development by the transcription factor Foxp3. Science. 2003; 299:1057–1061. [PubMed: 12522256]
8. Fontenot JD, Gavin MA, Rudensky AY. Foxp3 programs the development and function of CD4$^+$CD25$^+$ regulatory T cells. Nat Immunol. 2003; 4:330–336. [PubMed: 12612578]
9. Wing K, Onishi Y, Prieto-Martin P, Yamaguchi T, Miyara M, Fehervari Z, Nomura T, Sakaguchi S. CTLA-4 control over Foxp3$^+$ regulatory T cell function. Science. 2008; 322:271–275. [PubMed: 18845758]
10. Rubtsov YP, Rasmussen JP, Chi EY, Fontenot J, Castelli L, Ye X, Treuting P, Siewe L, Roers A, Henderson WR Jr, Muller W, Rudensky AY. Regulatory T cell-derived interleukin-10 limits inflammation at environmental interfaces. Immunity. 2008; 28:546–558. [PubMed: 18387831]
11. Curotto de Lafaille MA, Kutchukhidze N, Shen S, Ding Y, Yee H, Lafaille JJ. Adaptive Foxp3$^+$ regulatory T cell-dependent and -independent control of allergic inflammation. Immunity. 2008; 29:114–126. [PubMed: 18617425]
12. Wohlfert E, Belkaid Y. Role of endogenous and induced regulatory T cells during infections. J Clin Immunol. 2008; 28:707–715. [PubMed: 18810611]
13. Rouse BT, Sarangi PP, Suvas S. Regulatory T cells in virus infections. Immunol Rev. 2006; 212:272–286. [PubMed: 16903920]
14. Belkaid Y, Rouse BT. Natural regulatory T cells in infectious disease. Nat Immunol. 2005; 6:353–360. [PubMed: 15785761]
15. Scott-Browne JP, Shafiani S, Tucker-Heard G, Ishida-Tsubota K, Fontenot JD, Rudensky AY, Bevan MJ, Urdahl KB. Expansion and function of Foxp3-expressing T regulatory cells during tuberculosis. J Exp Med. 2007; 204:2159–2169. [PubMed: 17709423]
16. Fulton RB, Olson MR, Varga SM. Regulation of cytokine production by virus-specific CD8 T cells in the lungs. J Virol. 2008; 82:7799–7811. [PubMed: 18524828]
17. Sakaguchi S, Sakaguchi N, Asano M, Itoh M, Toda M. Immunologic self-tolerance maintained by activated T cells expressing IL-2 receptor alpha-chains (CD25). Breakdown of a single mechanism of self-tolerance causes various autoimmune diseases. J Immunol. 1995; 155:1151–1164. [PubMed: 7636184]
18. Olson MR, Hartwig SM, Varga SM. The number of respiratory syncytial virus (RSV)-specific memory CD8 T cells in the lung is critical for their ability to inhibit RSV vaccine-enhanced pulmonary eosinophilia. J Immunol. 2008; 181:7958–7968. [PubMed: 19017987]
19. McKinley L, Logar AJ, McAllister F, Zheng M, Steele C, Kolls JK. Regulatory T cells dampen pulmonary inflammation and lung injury in an animal model of pneumocystis pneumonia. J Immunol. 2006; 177:6215–6226. [PubMed: 17056551]
20. Mills KH. Regulatory T cells: friend or foe in immunity to infection? Nat Rev Immunol. 2004; 4:841–855. [PubMed: 15516964]
21. Ruckwardt TJ, Bonaparte KL, Nason MC, Graham BS. Regulatory T cells promote early influx of CD8$^+$ T cells in the lungs of respiratory syncytial virus-infected mice and diminish immunodominance disparities. J Virol. 2009; 83:3019–3028. [PubMed: 19153229]
22. Olson MR, Varga SM. CD8 T cells inhibit respiratory syncytial virus (RSV) vaccine-enhanced disease. J Immunol. 2007; 179:5415–5424. [PubMed: 17911628]
23. Nishioka T, Shimizu J, Iida R, Yamazaki S, Sakaguchi S. CD4$^+$CD25$^+$Foxp3$^+$ T cells and CD4$^+$CD25$^-$Foxp3$^+$ T cells in aged mice. J Immunol. 2006; 176:6586–6593. [PubMed: 16709816]

24. Lawrence CW, Ream RM, Braciale TJ. Frequency, specificity, and sites of expansion of CD8+ T cells during primary pulmonary influenza virus infection. J Immunol. 2005; 174:5332–5340. [PubMed: 15843530]
25. Taylor MD, Harris A, Babayan SA, Bain O, Culshaw A, Allen JE, Maizels RM. CTLA-4 and $CD4^+$ $CD25^+$ regulatory T cells inhibit protective immunity to filarial parasites in vivo. J Immunol. 2007; 179:4626–4634. [PubMed: 17878360]
26. Li MO, Wan YY, Flavell RA. T cell-produced transforming growth factor-beta1 controls T cell tolerance and regulates Th1- and Th17-cell differentiation. Immunity. 2007; 26:579–591. [PubMed: 17481928]
27. Malek TR. The biology of interleukin-2. Annu Rev Immunol. 2008; 26:453–479. [PubMed: 18062768]
28. Fontenot JD, Rasmussen JP, Gavin MA, Rudensky AY. A function for interleukin 2 in Foxp3-expressing regulatory T cells. Nat Immunol. 2005; 6:1142–1151. [PubMed: 16227984]
29. Fontenot JD, Rasmussen JP, Williams LM, Dooley JL, Farr AG, Rudensky AY. Regulatory T cell lineage specification by the forkhead transcription factor foxp3. Immunity. 2005; 22:329–341. [PubMed: 15780990]
30. Huehn J, Siegmund K, Lehmann JC, Siewert C, Haubold U, Feuerer M, Debes GF, Lauber J, Frey O, Przybylski GK, Niesner U, de la Rosa M, Schmidt CA, Brauer R, Buer J, Scheffold A, Hamann A. Developmental stage, phenotype, and migration distinguish naive- and effector/memory-like $CD4^+$ regulatory T cells. J Exp Med. 2004; 199:303–313. [PubMed: 14757740]
31. Friedline RH, Brown DS, Nguyen H, Kornfeld H, Lee J, Zhang Y, Appleby M, Der SD, Kang J, Chambers CA. $CD4^+$ regulatory T cells require CTLA-4 for the maintenance of systemic tolerance. J Exp Med. 2009; 206:421–434. [PubMed: 19188497]
32. Takahashi T, Tagami T, Yamazaki S, Uede T, Shimizu J, Sakaguchi N, Mak TW, Sakaguchi S. Immunologic self-tolerance maintained by $CD25^+CD4^+$ regulatory T cells constitutively expressing cytotoxic T lymphocyte-associated antigen 4. J Exp Med. 2000; 192:303–310. [PubMed: 10899917]
33. Read S, Malmstrom V, Powrie F. Cytotoxic T lymphocyte-associated antigen 4 plays an essential role in the function of $CD25^+CD4^+$ regulatory cells that control intestinal inflammation. J Exp Med. 2000; 192:295–302. [PubMed: 10899916]
34. Lehmann J, Huehn J, de la Rosa M, Maszyna F, Kretschmer U, Krenn V, Brunner M, Scheffold A, Hamann A. Expression of the integrin alpha Ebeta 7 identifies unique subsets of $CD25^+$ as well as $CD25^-$ regulatory T cells. Proc Natl Acad Sci U S A. 2002; 99:13031–13036. [PubMed: 12242333]
35. Xu B, Wagner N, Pham LN, Magno V, Shan Z, Butcher EC, Michie SA. Lymphocyte homing to bronchus-associated lymphoid tissue (BALT) is mediated by L-selectin/PNAd, $\alpha_4\beta_1$ integrin/VCAM-1, and LFA-1 adhesion pathways. J Exp Med. 2003; 197:1255–1267. [PubMed: 12756264]
36. Belkaid Y, Piccirillo CA, Mendez S, Shevach EM, Sacks DL. $CD4^+CD25^+$ regulatory T cells control Leishmania major persistence and immunity. Nature. 2002; 420:502–507. [PubMed: 12466842]
37. Olson MR, Varga SM. Pulmonary immunity and immunopathology: lessons from respiratory syncytial virus. Expert Rev Vaccines. 2008; 7:1239–1255. [PubMed: 18844597]
38. Graham BS, Bunton LA, Wright PF, Karzon DT. Role of T lymphocyte subsets in the pathogenesis of primary infection and rechallenge with respiratory syncytial virus in mice. J Clin Invest. 1991; 88:1026–1033. [PubMed: 1909350]
39. Suvas S, Kumaraguru U, Pack CD, Lee S, Rouse BT. $CD4^+CD25^+$ T cells regulate virus-specific primary and memory $CD8^+$ T cell responses. J Exp Med. 2003; 198:889–901. [PubMed: 12975455]
40. Haeryfar SM, DiPaolo RJ, Tscharke DC, Bennink JR, Yewdell JW. Regulatory T cells suppress $CD8^+$ T cell responses induced by direct priming and cross-priming and moderate immunodominance disparities. J Immunol. 2005; 174:3344–3351. [PubMed: 15749866]

41. Rai D, Pham NL, Harty JT, Badovinac VP. Tracking the total CD8 T cell response to infection reveals substantial discordance in magnitude and kinetics between inbred and outbred hosts. J Immunol. 2009; 183:7672–7681. [PubMed: 19933864]
42. Drake DR 3rd, Ream RM, Lawrence CW, Braciale TJ. Transient loss of MHC class I tetramer binding after $CD8^+$ T cell activation reflects altered T cell effector function. J Immunol. 2005; 175:1507–1515. [PubMed: 16034088]
43. Rutigliano JA, Graham BS. Prolonged production of TNF-alpha exacerbates illness during respiratory syncytial virus infection. J Immunol. 2004; 173:3408–3417. [PubMed: 15322205]
44. McHugh RS, Whitters MJ, Piccirillo CA, Young DA, Shevach EM, Collins M, Byrne MC. $CD4^+CD25^+$ immunoregulatory T cells: gene expression analysis reveals a functional role for the glucocorticoid-induced TNF receptor. Immunity. 2002; 16:311–323. [PubMed: 11869690]
45. Banz A, Peixoto A, Pontoux C, Cordier C, Rocha B, Papiernik M. A unique subpopulation of $CD4^+$ regulatory T cells controls wasting disease, IL-10 secretion and T cell homeostasis. Eur J Immunol. 2003; 33:2419–2428. [PubMed: 12938218]
46. Ito T, Hanabuchi S, Wang YH, Park WR, Arima K, Bover L, Qin FX, Gilliet M, Liu YJ. Two functional subsets of $FOXP3^+$ regulatory T cells in human thymus and periphery. Immunity. 2008; 28:870–880. [PubMed: 18513999]
47. Hsieh CS, Liang Y, Tyznik AJ, Self SG, Liggitt D, Rudensky AY. Recognition of the peripheral self by naturally arising $CD25^+$ $CD4^+$ T cell receptors. Immunity. 2004; 21:267–277. [PubMed: 15308106]
48. Caramalho I, Lopes-Carvalho T, Ostler D, Zelenay S, Haury M, Demengeot J. Regulatory T cells selectively express toll-like receptors and are activated by lipopolysaccharide. J Exp Med. 2003; 197:403–411. [PubMed: 12591899]
49. Kurt-Jones EA, Popova L, Kwinn L, Haynes LM, Jones LP, Tripp RA, Walsh EE, Freeman MW, Golenbock DT, Anderson LJ, Finberg RW. Pattern recognition receptors TLR4 and CD14 mediate response to respiratory syncytial virus. Nat Immunol. 2000; 1:398–401. [PubMed: 11062499]
50. Hall JA, Bouladoux N, Sun CM, Wohlfert EA, Blank RB, Zhu Q, Grigg ME, Berzofsky JA, Belkaid Y. Commensal DNA limits regulatory T cell conversion and is a natural adjuvant of intestinal immune responses. Immunity. 2008; 29:637–649. [PubMed: 18835196]
51. Duan W, So T, Croft M. Antagonism of airway tolerance by endotoxin/lipopolysaccharide through promoting OX40L and suppressing antigen-specific $Foxp3^+$ T regulatory cells. J Immunol. 2008; 181:8650–8659. [PubMed: 19050285]
52. Liu J, Ruckwardt TJ, Chen M, Johnson TR, Graham BS. Characterization of respiratory syncytial virus M- and M2-specific CD4 T cells in a murine model. J Virol. 2009; 83:4934–4941. [PubMed: 19264776]
53. Lund JM, Hsing L, Pham TT, Rudensky AY. Coordination of early protective immunity to viral infection by regulatory T cells. Science. 2008; 320:1220–1224. [PubMed: 18436744]
54. Sarween N, Chodos A, Raykundalia C, Khan M, Abbas AK, Walker LS. $CD4^+CD25^+$ cells controlling a pathogenic CD4 response inhibit cytokine differentiation, CXCR3 expression, and tissue invasion. J Immunol. 2004; 173:2942–2951. [PubMed: 15322152]
55. Lindell DM, Lane TE, Lukacs NW. CXCL10/CXCR3-mediated responses promote immunity to respiratory syncytial virus infection by augmenting dendritic cell and $CD8^+$ T cell efficacy. Eur J Immunol. 2008; 38:2168–2179. [PubMed: 18624292]
56. Castilow EM, Varga SM. Overcoming T cell-mediated immunopathology to achieve safe RSV vaccination. Future Virol. 2008; 3:445–454. [PubMed: 19057653]
57. Falsey AR, Hennessey PA, Formica MA, Cox C, Walsh EE. Respiratory syncytial virus infection in elderly and high-risk adults. N Engl J Med. 2005; 352:1749–1759. [PubMed: 15858184]
58. Collins PL, Graham BS. Viral and host factors in human respiratory syncytial virus pathogenesis. J Virol. 2008; 82:2040–2055. [PubMed: 17928346]
59. Peebles RS Jr, Graham BS. Pathogenesis of respiratory syncytial virus infection in the murine model. Proc Am Thorac Soc. 2005; 2:110–115. [PubMed: 16113477]

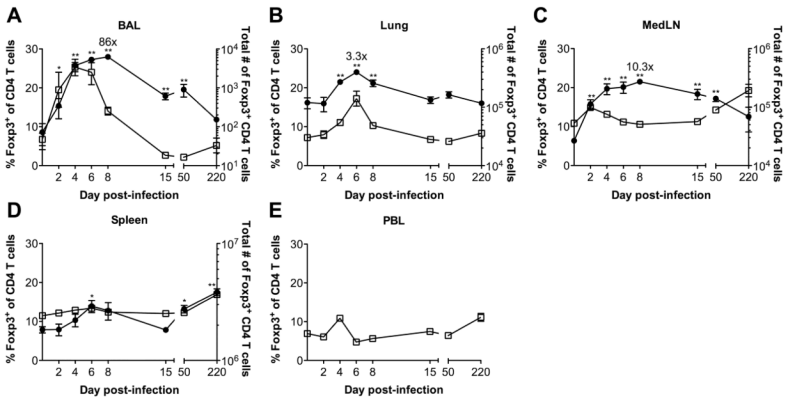

FIGURE 1.

Foxp3$^+$ Tregs accumulate in the lungs and medLNs following RSV infection. BALB/c mice were infected with RSV i.n. and cells from the BAL (A), lung parenchyma (B), medLNs (C), spleen (D), and PBL (E) were collected at the indicated times. The percentage of CD4 T cells that are Foxp3$^+$ (open squares, left y-axis) and the total number of Foxp3$^+$ CD4 T cells (filled circles, right y-axis) were determined by flow cytometry. In (E), only the percentage of CD4 T cells that are Foxp3$^+$ is shown. Numbers in the plots represent the fold-increase in the total number of Foxp3$^+$ Tregs over naïve controls. The data for the spleen, medLN, and PBL represent the mean ± SEM from 2 separate experiments at each time point with n=4 mice per experiment except for day 50, which represents 3 separate experiments. Data for the lung parenchyma and BAL represent data from 2 separate experiments on days 2, 8, 15, and 220; 3 experiments on days 0, 4, 50; and 4 experiments on day 6. BAL was pooled from 4 mice per experiment and divided by 4 to determine the total number of cells. Statistical analysis of total numbers of Tregs compared to baseline (day 0) numbers was done on $\log_{10}$-transformed data using one-way ANOVA with Dunnett post-tests. *, p<0.05; **, p<0.01.

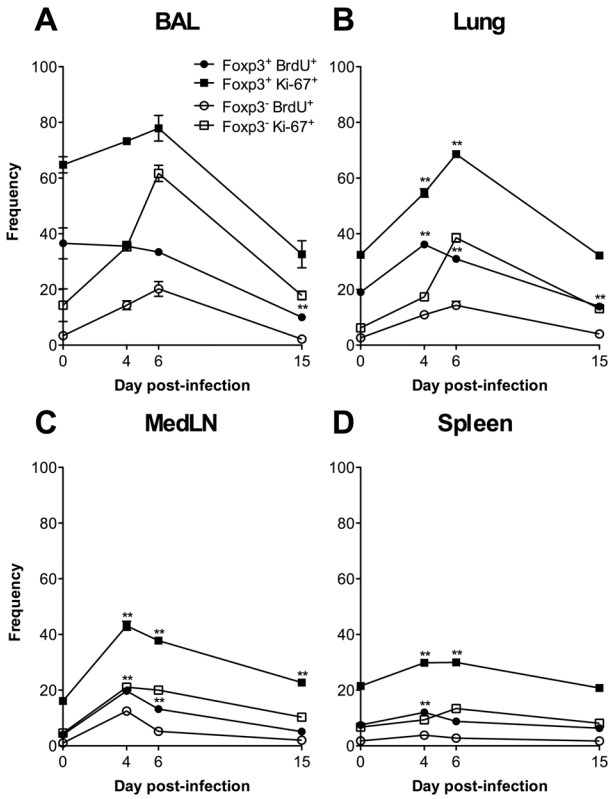

FIGURE 2.

Foxp3$^+$ Tregs proliferate in response to RSV infection. Naïve or RSV-infected BALB/c mice were administered BrdU i.p. and i.n. and cells were harvested 24 hrs later at the times indicated. The percentage of Foxp3$^-$ (open symbols) or Foxp3$^+$ (closed symbols) CD4 T cells that were BrdU$^+$ (circles) or Ki-67$^+$ (squares) is shown for Tregs from the BAL (A), lung parenchyma (B), medLNs (C), and spleen (D). Data represent the mean ± SEM from 4 separate experiments for BrdU data and 2 separate experiments for Ki-67 data at each time point with *n*=4 mice per experiment. BAL was pooled from 4 mice per experiment. Statistical analysis of the frequencies of BrdU$^+$ or Ki-67$^+$ Foxp3$^+$ Tregs compared to baseline levels (day 0) was done using one-way ANOVA with Dunnett post-tests. **, $p<0.01$.

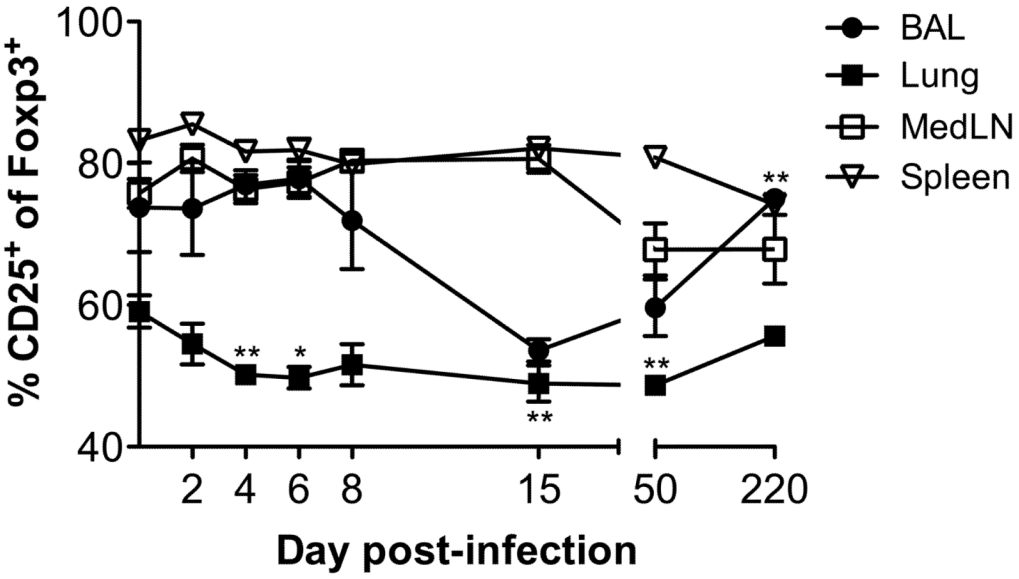

FIGURE 3.

Foxp3$^+$ Tregs modulate CD25 expression following RSV infection. BALB/c mice were infected with RSV i.n. and the percentage of Foxp3$^+$ Tregs expressing CD25 in the BAL, lung parenchyma, medLNs, and spleen was determined at the times indicated. Data represent the mean ± SEM from 2–3 separate experiments except for data from day 220, which represents a single experiment. There were n=4 mice per experiment at each time point. BAL was pooled from 4 mice per experiment. Statistical analysis of the frequencies of CD25$^+$ Tregs compared to baseline levels (day 0) was done using one-way ANOVA with Dunnett post-tests. *, p<0.05; **, p<0.01.

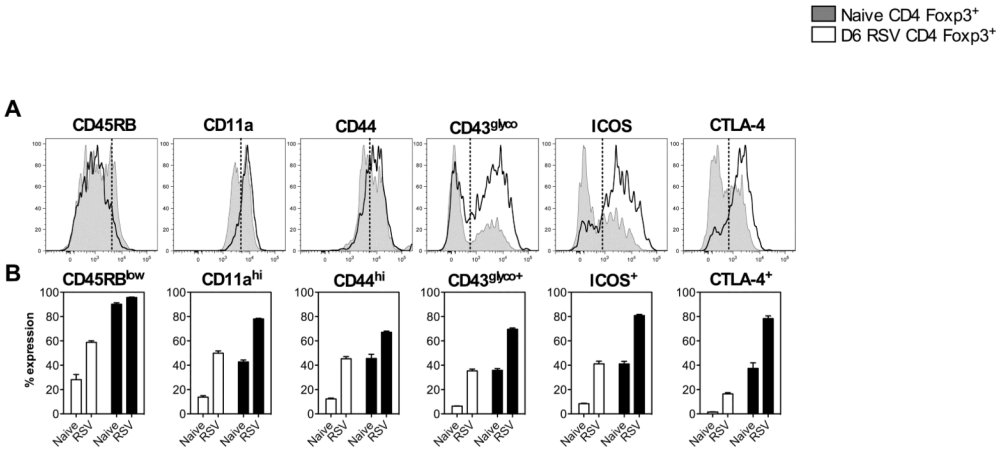

FIGURE 4.

Pulmonary Tregs acquire an activated phenotype following RSV infection. Cells from the lung parenchyma (post-BAL) were stained for various markers and intracellular Foxp3. (A) Histogram plots are gated on Foxp3$^+$ CD4 T cells from naïve mice (grey shaded) or from mice infected with RSV 6 days earlier (solid line). Vertical dotted lines indicate where gates were drawn based on isotype staining (CD43^{glyco}, ICOS, and CTLA-4) or for CD45RB, CD11a, and CD44 expression. CD43^{glyco} is the activation-associated glycoform of CD43. Plots are representative of data from 2 separate experiments. (B) Cumulative data from histograms showing marker expression by Foxp3$^-$ (□) and Foxp3$^+$ (▪) CD4 T cells from the lungs of naïve or RSV-infected lungs 6 days p.i. Error bars represent the SEM. Data were analyzed using Welch corrected unpaired *t* tests. Relative to naïve mice within each subset (Foxp3$^-$ or Foxp3$^+$), all changes in percent expression of markers in RSV-infected mice were statistically significant ($p<0.01$).

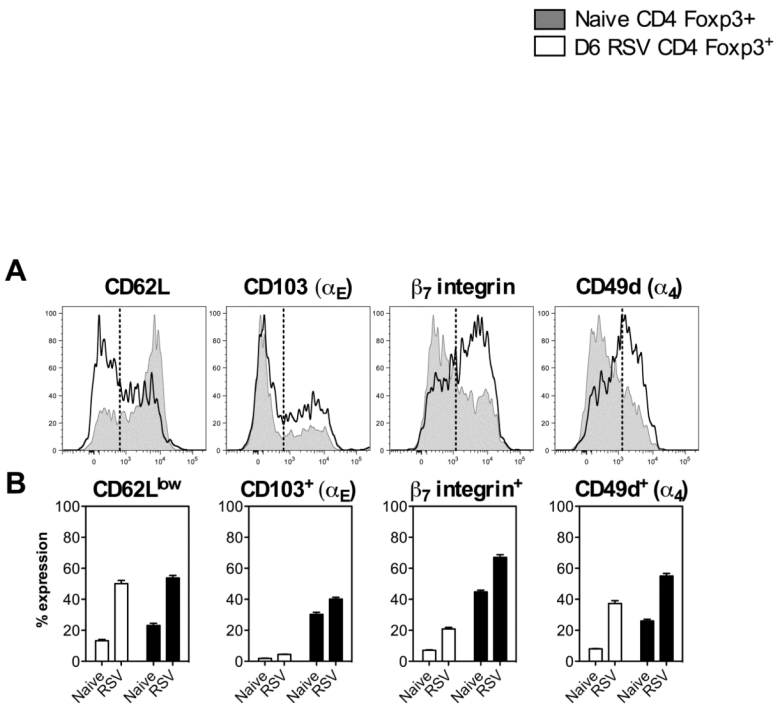

FIGURE 5.

Pulmonary Tregs modulate trafficking molecules following RSV infection. Cells from the lung parenchyma (post-BAL) were stained for various extracellular markers and intracellular Foxp3. (A) Histogram plots are gated on $Foxp3^+$ CD4 T cells from naïve mice (grey shaded) or from mice infected with RSV 6 days earlier (solid line). Vertical dotted lines indicate where gates were drawn based on isotype staining (CD62L and CD103) or for β7 and CD49d expression. Plots are representative of data from 2 separate experiments. (B) Cumulative data from histograms showing marker expression by $Foxp3^-$ (□) and $Foxp3^+$ (▪) CD4 T cells from the lungs of naïve or RSV-infected lungs 6 days p.i. Error bars represent the SEM. Data were analyzed using Welch corrected unpaired *t* tests. Relative to naïve mice within each subset ($Foxp3^-$ or $Foxp3^+$), all changes in percent expression of markers in RSV-infected mice were statistically significant ($p<0.01$).

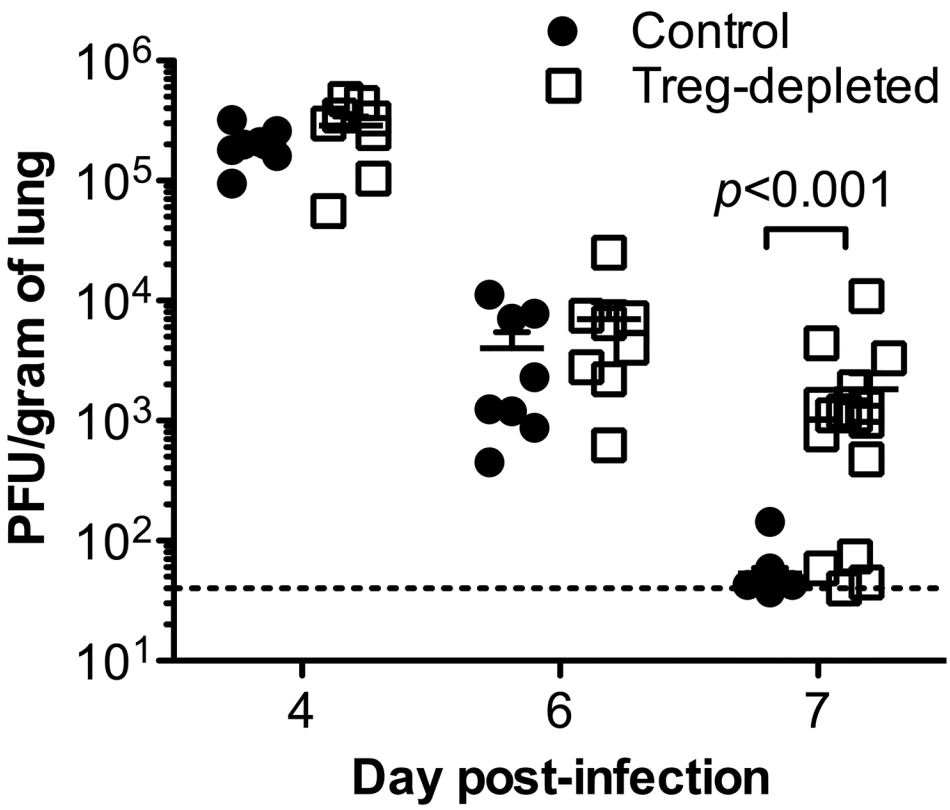

FIGURE 6.

Depletion of Tregs delays virus clearance. Tregs were depleted in BALB/c mice with anti-CD25 mAb (clone PC61) treatment as described in Materials and Methods. Control mice received rat IgG. Following infection with RSV, virus titers were measured in the lungs of control or Treg-depleted mice. The dashed line represents the limit of detection. Data represent 2 separate experiments for day 4 and 6 p.i. and 4 separate experiments for day 7 p.i. with *n*=4 mice per experiment. Error bars represent the SEM. Data were analyzed using nonparametric Mann-Whitney *U* tests.

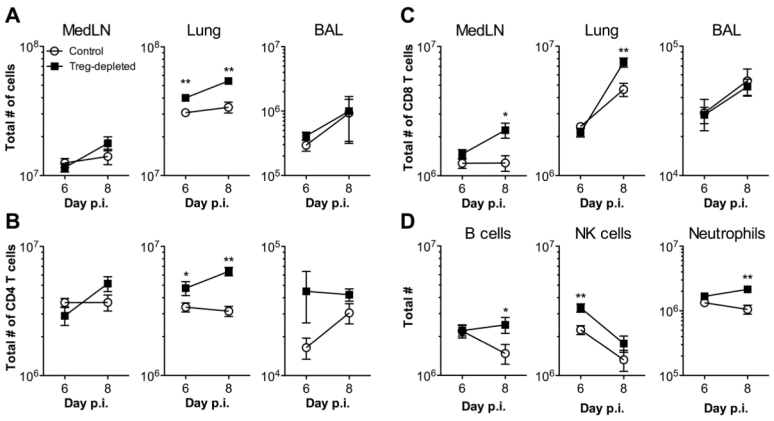

FIGURE 7.

Total numbers of cells in the medLNs, lung parenchyma, and BAL of control or Treg-depleted mice. BALB/c mice were depleted of Tregs prior to acute RSV infection. Total numbers of cells (A), CD4 T cells (B), and CD8 T cells (C) in the medLNs, lung parenchyma, and BAL were determined in control or Treg-depleted mice on days 6 and 8 p.i. (D) Total numbers of B cells ($CD19^+B220^+$), NK cells ($CD3^-DX5^+$), and neutrophils ($Ly6C^+Ly6G^+CD11b^+$) were enumerated by flow cytometry in the lungs (post-BAL) 6 and 8 days p.i. Data in (A) and (C) represent 5 experiments on day 6 p.i. and 2 experiments on day 8 p.i. with n=4 mice per experiment. Data in (B) and (D) represent 2 experiments with n=4 mice per experiment. Error bars represent the SEM. All data were $\log_{10}$ transformed prior to statistical analysis with unpaired t tests. *, $p<0.05$; **, $p<0.01$.

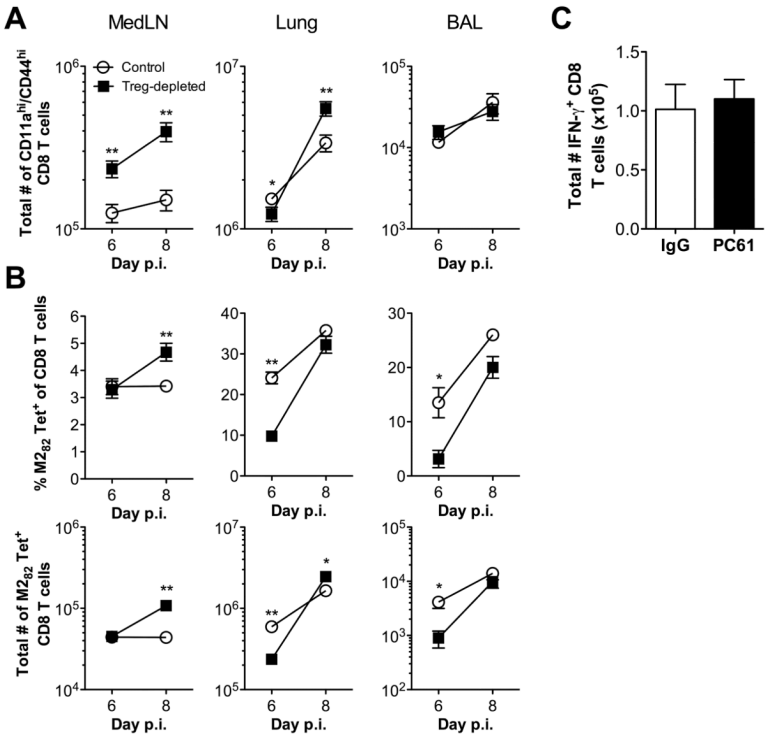

FIGURE 8.

Decreased early recruitment of RSV-specific CD8 T cells into the lungs in Treg-depleted mice. BALB/c mice were depleted of Tregs prior to acute RSV infection. (A) Total numbers of $CD11a^{hi}CD44^{hi}$ CD8 T cells were determined in the medLNs, lung parenchyma, and BAL 6 and 8 days p.i. Cells from the medLNs and lung parenchyma of naïve mice were used to determine the gating for $CD11a^{hi}CD44^{hi}$ CD8 T cells in RSV-infected mice. Data represent 5 experiments on day 6 p.i. and 2 experiments on day 8 p.i. with *n*=4 mice per experiment. (B) Frequency (top) and total numbers (bottom) of $M2_{82\text{-}90}$ tetramer^{+} CD8 T cells in the medLNs, lung parenchyma, and BAL 6 and 8 days p.i. MedLNs and lungs from naïve mice were used as controls for tetramer staining. Data represent 3 experiments on day 6 p.i. and 2 experiments on day 8 p.i. with *n*=4 mice per experiment. (C) Total numbers of IFN-γ^{+} $M2_{82\text{-}90}$-specific CD8 T cells in the spleen 6 days p.i. Data represent 2 experiments with *n*=4 mice per experiment. Error bars represent the SEM. Data were analyzed using unpaired *t* tests. Data were $\log_{10}$-transformed except for the top panel of (B) prior to analysis. *, $p<0.05$; **, $p<0.01$.

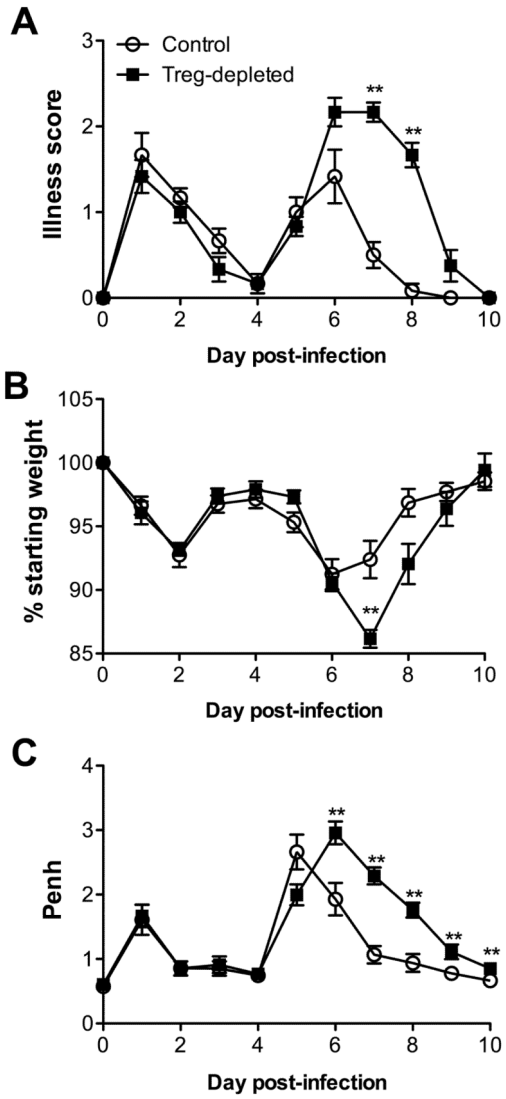

Figure 9.

Depletion of Tregs exacerbates the severity of RSV-induced disease. BALB/c mice were depleted of Tregs prior to acute RSV infection. Mice were monitored daily for clinical illness (A), weight loss (B), and airway resistance (Penh) (C). Airway resistance was assessed using a whole body plethysmograph. Data represent the mean ± SEM from 3 separate experiments with n=4 mice per experiment. Statistical analysis found a difference in weight loss and Penh (p=0.0001 and p<0.0001, respectively) in the overall trends between control and Treg-depleted mice using two-way repeated-measures ANOVA. Individual days in (A-C) were analyzed using nonparametric Mann-Whitney U tests. **, p<0.01.

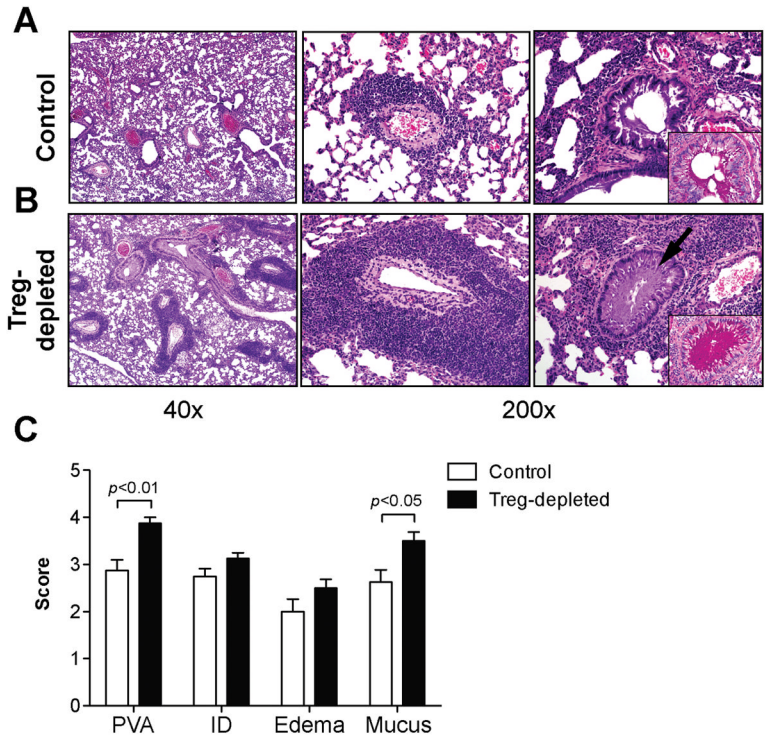

Figure 10.

Increased inflammation and mucus in the lungs of Treg-depleted mice. Whole lungs from control (A) or Treg-depleted mice (B) were collected, sectioned and either H&E or PAS stained. Sections were scored for perivascular aggregates of leukocytes (PVA), interstitial disease (ID), edema and mucus. On low magnification (40x), control and Treg-depleted mice were distinguished by prominent perivascular inflammation (left panels) that was mostly composed of lymphoid cells (middle panels, 200x magnification). Treg-depleted mice also had severe mucinous changes (right panels) with some airways completely obstructed by mucus (arrow). Insets in the right panels are PAS-stained serial sections that highlight magenta stained mucus in the airway lumen. (C) Cumulative histological scores. Images (A and B) and scores (C) are representative of 8 mice per group. All data were analyzed using nonparametric Mann-Whitney *U* tests.

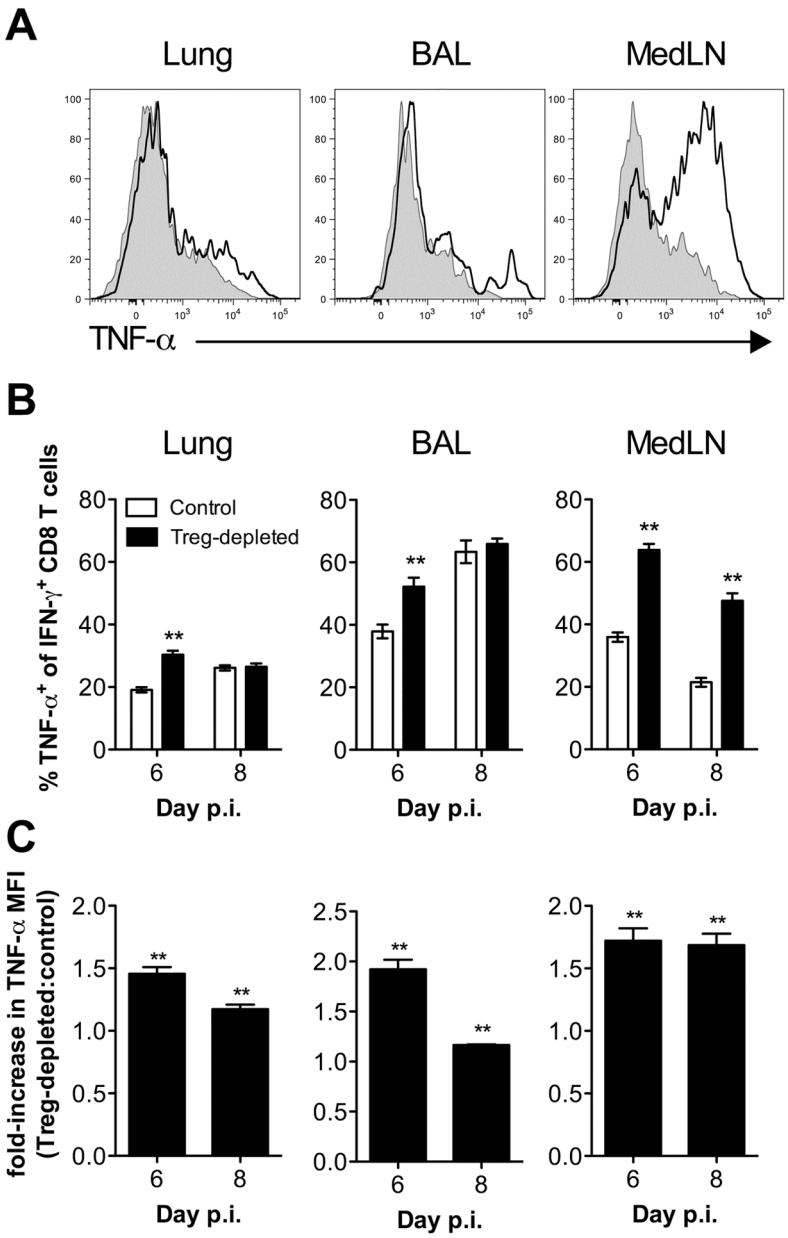

Figure 11.

Increased TNF-α production by virus-specific CD8 T cells in the lungs, medLNs, and spleens of Treg-depleted mice. On days 6 and 8 p.i. cells from the lung parenchyma, BAL, and medLNs were stimulated directly *ex vivo* with $M2_{82\text{-}90}$ peptide and stained for intracellular IFN-γ and TNF-α. (A) TNF-α production by $M2_{82\text{-}90}$-specific CD8 T cells on day 6 p.i. Histograms are gated on IFN-γ^+ CD8 T cells from control (grey shaded) or Treg-depleted mice (solid line). Histograms are representative of 5 separate experiments. (B) Percent of IFN-γ_+ CD8 T cells that co-produced TNF-α. (C) Fold-increase in the TNF-α geometric MFI in Treg-depleted mice over control mice. To calculate the fold-increase, the geometric MFI was compared between groups within each experiment. Data in (B and C) represent the mean ± SEM from 5 experiments for day 6 p.i. and 3 experiments for day 8 p.i. with n=4 mice per experiment. Data in (B) were analyzed using unpaired t tests. Data in (C) were analyzed using a two-way ANOVA on $\log_{10}$-transformed data. *p<0.05; **, p<0.01.